Journal of Engineering and Computer Sciences, Qassim University, Vol. 3, No. 1, pp. 11-25 (January 2010/Muharram 1431H)

Direct Torque Control of Dual Three Phase Inverter Fed Six Phase Induction Motor Drive

S. A. Zaid*, O. A. Mahgoub, K. Emetwally, and S. E. Abo-Shady

Dept. of Electrical Power and Machines, Faculty of Engineerung,
Cairo University, Giza, Egypt
** sherifzaid@yahoo.com*

(Received 21/1/2009, accepted for publication 1/11/2009)

ABSTRACT. Six-phase induction motor “IM” has advantages over three phase“3-φ”IM like lower harmonics, lower losses, improved reliability, higher torque per ampere, and higher power rating drive. However the control of such motors is more complex than that of the 3-φ□motors. The principles of direct torque control “DTC”, which is a well-known control method for 3-φ□motors, can be utilized to overcome this complexity. This paper introduces the application of the DTC principles to 6-φ□□IMs drives. The whole 6-φ□IM drive system is modeled and simulated in the stationary reference frame. However, it is noted from circuit analysis and Matlab simulations that the use of the conventional 6-φ□inverter gives poor performance drive. This is due to the fact that with the conventional inverter only six switching states can give balanced output voltages instead of 64 switching states. This results in lower capability of control, less utilization of the DC supply, and more harmonic distortion as well. However to avoid this demerits, the authors have inferred that the use of a dual 3-φ inverter is the solution to be adapted. Simulation results of a DTC 6-φ□IM drive show improved performance compared with the performance of the field orientation trials in the literature.

KEYWORDS: Six-phase “6-φ□”, induction motor “IM”, direct torque control “DTC”, voltage source inverter “VSI”.

LIST OF SYMBOLS AND ABBREVIATIONS

A-B-C-D-E-F	The six phases notations
d-q	Direct-quadrature frame (stator frame)
d-q-z_1-z_2-o_1-o_2	The six phases notations after transformation to stationary frame
C, C_1	Constants
$C(\,)$	Abbreviation of cosine
i_{ds}, i_{qs}	The stator current components in the stator reference frame
i_{dr}, i_{qr}	The rotor current components in the stator reference frame
$[I]$	The identity matrix
L_m	Maximum value of the mutual inductance bet. rotor and stator
L_r, L_s	Rotor and stator inductances referred to stator
L_{lr}, L_{ls}	Rotor and stator leakage inductances referred to stator
$[L_{ss}]$	The stator self-inductance matrix
$[L_{rr}]$	The rotor self-inductance matrix referred to stator
$[L_{sr}]$	The stator-rotor mutual-inductance matrix referred to stator
N	The sector number
P	Differentiation w.r.t time
P	Number of poles
R_s, R_r	Stator and rotor resistances referred to stator
S_A, S_B, S_C, S_D, S_E, S_F	6-ϕ Inverter switching logic functions
T	Motor developed torque
T^*	The reference torque
T	Time
T_L	Rated motor torque
$[T]$	The six phase transformation matrix to stationary frame
$[T_r^s]$	The six phase transformation matrix to a rotating frame
V_{dc}	Inverter DC supply voltage
v_{an}, v_{bn}, v_{cn}	The stator phase voltages
V_{As}, V_{Bs}, V_{Cs}, V_{Ds}, V_{Es}, V_{Fs}	The six inverter phase voltages w.r.t the load neutral point
V_{AN}, V_{BN}, V_{CN}, V_{DN}, V_{EN}, V_{FN}	The six inverter phase voltages w.r.t the DC supply ground
ω^*	The motor reference speed
θ	The rotor angular position w.r.t. the d-axis
ΔT	Torque error
$\Delta\lambda$	Flux error
λ^*	The stator flux vector in the stator frame
λ_q,λ_d	The stator flux components in the stator reference frame

1. Introduction

It is generally known that balanced poly-phase voltages applied to a corresponding balanced winding result in a rotating magnetic field. In an ideal machine having a sinusoidal distribution of the air gap flux of a given peak density, the operating c/c's would be identical for any number of phases greater than one. Very early IM's had two phases, but the 3-φ version very soon replaced these. Three-phase version eliminated 3rd harmonic problems and resulted in a motor which was generally better. Increasing the number of phases beyond three has advantages, which might be worth considering for certain applications [1]. Key advantages of multiphase IM drive systems over conventional 3-φ systems are summarized as follows:

1. Reduction of the required inverter phase current permits the use of a single power device for each inverter switch instead of a group of devices connected in parallel. Problems of static and dynamic current sharing among parallel devices, such as bipolar transistors, are thereby eliminated in large drive systems [2].
2. The sixth harmonic pulsating torques, associated with the conventional 3-φ IM drives that fed from six-step VSI, is eliminated by the appropriate choice of a multiphase motor winding configuration [2].
3. Rotor harmonic losses are reduced compared with the level produced in 3-φ systems [2].
4. The total system reliability is improved by providing continued system operation with degraded performance following loss of excitation to one of the machine stator phases [2].
5. The torque per ampere for the same-size machine is increased [3].
6. A high power rating drive can be obtained with standard inverter power modules due to the use of more modules of lower rating [4].

The high phase order drive is likely to remain limited to specialized applications, where high reliability is demanded such as electric/hybrid vehicles, aerospace applications, ship propulsion, and high power drive applications.

However, when a multiphase system is implemented with the conventional voltage source inverter, large harmonic currents have been observed [2], [5], [6], and [7]. This is due to misunderstanding of the inverter modes. Attempts have been made to improve the six phase drive performance by introducing alternative modulation schemes [8-10]. The conventional topology of the 6-φ inverter essentially gives low performance drive and poor utilization of the DC supply. A new topology for the 6-φ inverter will be introduced in the present paper to improve the system performance.

Field orientation control strategy has been applied to multiphase IM [3, 5& 11]. In this paper, the concept of DTC is applied to 6-ϕ IM, as there is no previous attempt in the literature.

2. Machine Model

In a 6-φ IM, the six-stator phases are distributed with a spacing of 60°. The following normal assumptions have been made in deriving the 6-φ IM model:

1. Machine windings are of sinusoidal distribution.
2. Saturation is neglected.
3. Mutual leakage inductances are neglected.

Under these assumptions the voltage equations of the machine, in the original six dimensional space, can be derived.

2.1 Machine Model in the Original Six Dimensional Space

The machine stator and rotor voltage equations can be written as:

$$[V_s]=[R_s]\cdot[I_s]+p\cdot([L_{ss}]\cdot[I_s]+[L_{sr}]\cdot[I_r]) \tag{1}$$

$$[V_r]=[R_r]\cdot[I_r]+p\cdot([L_{rr}]\cdot[I_r]+[L_{rs}]\cdot[I_s]) \tag{2}$$

Where, in these equations, the voltage and current vectors are defined as:

$$[V]_s=\begin{bmatrix}v_{As}\\v_{Bs}\\v_{Cs}\\v_{Ds}\\v_{Es}\\v_{Fs}\end{bmatrix},\quad [I]_s=\begin{bmatrix}i_{As}\\i_{Bs}\\i_{Cs}\\i_{Ds}\\i_{Es}\\i_{Fs}\end{bmatrix},\quad [V]_r=\begin{bmatrix}v_{Ar}\\v_{Br}\\v_{Cr}\\v_{Dr}\\v_{Er}\\v_{Fr}\end{bmatrix},\quad [I]_r=\begin{bmatrix}i_{Ar}\\i_{Br}\\i_{Cr}\\i_{Dr}\\i_{Er}\\i_{Fr}\end{bmatrix} \tag{3}$$

The resistance and inductance matrices in Eq.(1) and Eq.(2) are given in Appendix I.

2.2 Transformation of the Voltage Equations to a New Reference Frame

Modeling and control of 6-ϕ machine can be simplified with a proper transformation to a six dimensional frame of reference [5]. The transformation matrix used will be represented by six vectors and referred to as the space "d-q-z_1-z_2-o_1-o_2" [12].

$$[T] = \frac{1}{\sqrt{3}}\begin{bmatrix} 1 & .5 & -.5 & -1 & -.5 & .5 \\ 0 & \frac{\sqrt{3}}{2} & \frac{\sqrt{3}}{2} & 0 & \frac{-\sqrt{3}}{2} & \frac{-\sqrt{3}}{2} \\ 1 & -.5 & -.5 & 1 & -.5 & -.5 \\ 0 & \frac{-\sqrt{3}}{2} & \frac{\sqrt{3}}{2} & 0 & \frac{-\sqrt{3}}{2} & \frac{\sqrt{3}}{2} \\ \frac{1}{\sqrt{2}} & \frac{-1}{\sqrt{2}} & \frac{1}{\sqrt{2}} & \frac{-1}{\sqrt{2}} & \frac{1}{\sqrt{2}} & \frac{-1}{\sqrt{2}} \\ \frac{1}{\sqrt{2}} & \frac{1}{\sqrt{2}} & \frac{1}{\sqrt{2}} & \frac{1}{\sqrt{2}} & \frac{1}{\sqrt{2}} & \frac{1}{\sqrt{2}} \end{bmatrix} \tag{4}$$

The actual machine phases will be referred to as "*A-B-C-D-E-F*". The transformation transforms the original vector space to a new vector space having the following properties:

- Machine variable components that produce air gap flux are transformed to the *d-q* subspace. The *d-q* subspace, commonly referred to as the *d-q* plane, is electromechanical energy conversion related.
- Those components of machine variables, which will not produce air gap penetrating flux, will be mapped to the subspace z_1-z_2-o_1-o_2 by Eq.(4). These components can be classified as a new type of zero sequence subspace [11].

Applying transformation given by Eqn.(4) to Eqn.(1) and Eqn.(2) yields

$$\begin{bmatrix} v_{ds} \\ v_{qs} \\ v_{z_1s} \\ v_{z_2s} \\ v_{o_1s} \\ v_{o_2s} \end{bmatrix} = [R_s]\cdot\begin{bmatrix} i_{ds} \\ i_{qs} \\ i_{z_1s} \\ i_{z_2s} \\ i_{o_1s} \\ i_{o_2s} \end{bmatrix} + p\cdot\begin{bmatrix} L_{ls}+3L_m & 0 & 0 & 0 & 0 & 0 \\ 0 & L_{ls}+3L_m & 0 & 0 & 0 & 0 \\ 0 & 0 & L_{ls} & 0 & 0 & 0 \\ 0 & 0 & 0 & L_{ls} & 0 & 0 \\ 0 & 0 & 0 & 0 & L_{ls} & 0 \\ 0 & 0 & 0 & 0 & 0 & L_{ls} \end{bmatrix}\begin{bmatrix} i_{ds} \\ i_{qs} \\ i_{z_1s} \\ i_{z_2s} \\ i_{o_1s} \\ i_{o_2s} \end{bmatrix}$$
$$+\,3L_m\cdot\begin{bmatrix} \cos(\theta) & -\sin(\theta) & 0 & 0 & 0 & 0 \\ \sin(\theta) & \cos(\theta) & 0 & 0 & 0 & 0 \\ 0 & 0 & 0 & 0 & 0 & 0 \\ 0 & 0 & 0 & 0 & 0 & 0 \\ 0 & 0 & 0 & 0 & 0 & 0 \\ 0 & 0 & 0 & 0 & 0 & 0 \end{bmatrix}\begin{bmatrix} i_{dr} \\ i_{qr} \\ i_{z_1r} \\ i_{z_2r} \\ i_{o_1r} \\ i_{o_2r} \end{bmatrix} \tag{5}$$

$$\begin{bmatrix} 0 \\ 0 \\ 0 \\ 0 \\ 0 \\ 0 \end{bmatrix} = [R_r]\cdot\begin{bmatrix} i_{dr} \\ i_{qr} \\ i_{z_1r} \\ i_{z_2r} \\ i_{o_1r} \\ i_{o_2r} \end{bmatrix} + p\cdot\begin{bmatrix} L_{lr}+3L_m & 0 & 0 & 0 & 0 & 0 \\ 0 & L_{lr}+3L_m & 0 & 0 & 0 & 0 \\ 0 & 0 & L_{lr} & 0 & 0 & 0 \\ 0 & 0 & 0 & L_{lr} & 0 & 0 \\ 0 & 0 & 0 & 0 & L_{lr} & 0 \\ 0 & 0 & 0 & 0 & 0 & L_{lr} \end{bmatrix}\begin{bmatrix} i_{dr} \\ i_{qr} \\ i_{z_1r} \\ i_{z_2r} \\ i_{o_1r} \\ i_{o_2r} \end{bmatrix}$$
$$+\,3L_m\cdot\begin{bmatrix} \cos(\theta) & \sin(\theta) & 0 & 0 & 0 & 0 \\ -\sin(\theta) & \cos(\theta) & 0 & 0 & 0 & 0 \\ 0 & 0 & 0 & 0 & 0 & 0 \\ 0 & 0 & 0 & 0 & 0 & 0 \\ 0 & 0 & 0 & 0 & 0 & 0 \\ 0 & 0 & 0 & 0 & 0 & 0 \end{bmatrix}\begin{bmatrix} i_{ds} \\ i_{qs} \\ i_{z_1s} \\ i_{z_2s} \\ i_{o_1s} \\ i_{o_2s} \end{bmatrix} \tag{6}$$

Where θ is the rotor angular position.

As expected it is observed immediately from the above equations that all the electromechanical energy conversion related variable components are mapped into the *d-q* plane, and the non-electromechanical energy conversion related variable components are transformed to the z_1-z_2 and o_1-o_2 planes. Hence, the dynamic equations of the machine are totally decoupled. As a result the analysis and control of the machine can be greatly simplified. In the analysis just completed, *d-q* reference frames were, in effect, separately attached to the stator and rotor, rotating at zero and rotor angular speed, respectively. To express the stator and rotor equations in the same reference frame and thus eliminate the sine and the cosine terms in the above equations, the following relation transformation, which transforms the rotor variables to the stationary reference frame, is appropriate:

$$\left[T^s\right] = \begin{bmatrix} cos(\theta) & -sin(\theta) & 0 & 0 & 0 & 0 \\ sin(\theta) & cos(\theta) & 0 & 0 & 0 & 0 \\ 0 & 0 & 0 & 0 & 0 & 0 \\ 0 & 0 & 0 & 0 & 0 & 0 \\ 0 & 0 & 0 & 0 & 0 & 0 \\ 0 & 0 & 0 & 0 & 0 & 0 \end{bmatrix} \tag{7}$$

With this relation transformation applied to Eq.(5) and Eq.(6), the following stator and rotor combined *d-q* plane stationary reference frame equation results:

$$\begin{bmatrix} v_{ds} \\ v_{qs} \\ 0 \\ 0 \end{bmatrix} = \begin{bmatrix} R_s + L_s p & 0 & Mp & \omega M \\ 0 & R_s + L_s p & \omega M & Mp \\ Mp & \omega M & R_r + L_r p & \omega L_r \\ -\omega M & Mp & -\omega L_r & R_r + L_r p \end{bmatrix} \cdot \begin{bmatrix} i_{ds} \\ i_{qs} \\ i_{dr} \\ i_{qr} \end{bmatrix} \tag{8}$$

Where: $p = \frac{d}{dt}$, $L_s = L_{ls} + 3L_m$, $L_r = L_{lr} + 3L_m$, $M = 3L_m$

The electromagnetic torque is given by:

$$T = \frac{6}{2}\frac{P}{2} L_m \left(i_{qs} i_{dr} - i_{qr} i_{ds}\right) \tag{9}$$

3. Inverter Model and Space Vectors

A 6-φ voltage source inverter is shown in Fig.(1). This inverter operates with the same main rules as the 3-φ inverter (i.e. the two switches, or transistors, of any leg are always in opposite operation), and there are always six switches in conduction. The inputs to the inverter, as a control system building block, are the switching functions of the inverter switches (S_A, S_B, S_C, S_D, S_E, S_F). These functions are logic functions, equal '1' when the phase terminal is connected to the positive of the DC side, and equal '0' when the phase terminal is connected to the negative of the DC side. However, the outputs are the motor phase voltages (v_{As}, v_{Bs}, v_{Cs}, v_{Ds}, v_{Es}, v_{Fs}).

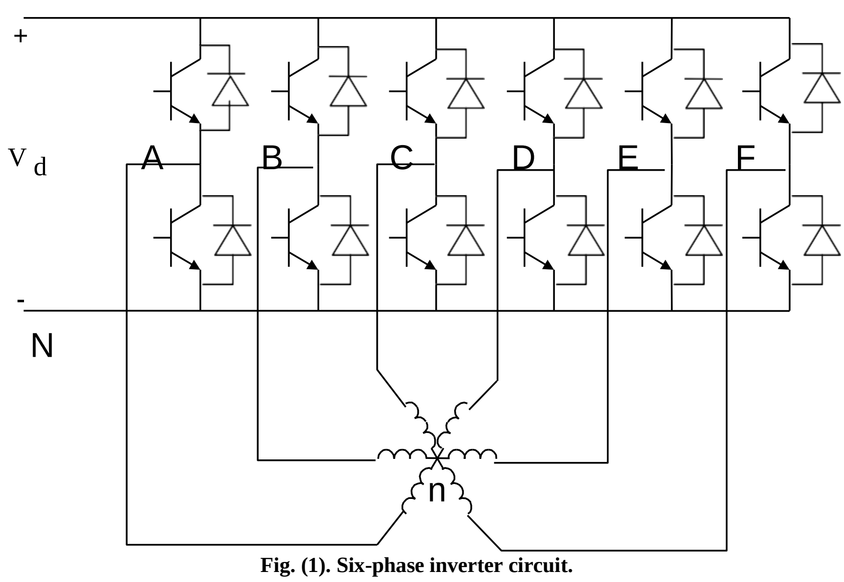

Fig. (1). Six-phase inverter circuit.

The model can be derived as follows. The inverter phase voltages (v_{AN}, v_{BN}, v_{CN}, v_{DN}, v_{EN}, v_{FN}), w.r.t the DC supply ground, can be derived from the switching states using:

$$\left(v_{AN}, v_{BN}, v_{CN} v_{DN}, v_{EN}, v_{FN}\right) = V_{dc}\left(S_A, S_B, S_C, S_D, S_E, S_F\right) \tag{10}$$

Then the motor phase voltages are derived from the inverter phase voltages by applying Kirchhoff laws to the inverter-motor circuit:

$$\begin{aligned} v_{As} - v_{Bs} &= v_{AN} - v_{BN} \\ v_{As} - v_{Cs} &= v_{AN} - v_{CN} \\ v_{As} - v_{Ds} &= v_{AN} - v_{DN} \\ v_{As} - v_{Es} &= v_{AN} - v_{EN} \\ v_{As} - v_{Fs} &= v_{AN} - v_{FN} \end{aligned} \tag{11}$$

$$v_{As} + v_{Bs} + v_{Cs} + v_{Ds} + v_{Es} + v_{Fs} = 0$$

Solving these equations then using (10)we get the input output relation for the nverter:

$$\begin{bmatrix} v_{As} \\ v_{Bs} \\ v_{Cs} \\ v_{Ds} \\ v_{Es} \\ v_{Fs} \end{bmatrix} = \frac{V_{dc}}{6} \begin{bmatrix} 5 & -1 & -1 & -1 & -1 & -1 \\ -1 & 5 & -1 & -1 & -1 & -1 \\ -1 & -1 & 5 & -1 & -1 & -1 \\ -1 & -1 & -1 & 5 & -1 & -1 \\ -1 & -1 & -1 & -1 & 5 & -1 \\ -1 & -1 & -1 & -1 & -1 & 5 \end{bmatrix} \begin{bmatrix} S_A \\ S_B \\ S_C \\ S_D \\ S_E \\ S_F \end{bmatrix} \tag{12}$$

The 6-φ voltage source inverter has a total of 64 switching states, shown in Table (1).

Table (1). The 6-ϕ single inverter switching states

	S_F	S_E	S_D	S_C	S_B	S_A		S_F	S_E	S_D	S_C	S_B	S_A
V_0	0	0	0	0	0	0	V_{32}	1	0	0	0	0	0
V_1	0	0	0	0	0	1	V_{33}	1	0	0	0	0	1
V_2	0	0	0	0	1	0	V_{34}	1	0	0	0	1	0
V_3	0	0	0	0	1	1	V_{35}	1	0	0	0	1	1
V_4	0	0	0	1	0	0	V_{36}	1	0	0	1	0	0
V_5	0	0	0	1	0	1	V_{37}	1	0	0	1	0	1
V_6	0	0	0	1	1	0	V_{38}	1	0	0	1	1	0
V_7	0	0	0	1	1	1	V_{39}	1	0	0	1	1	1
V_8	0	0	1	0	0	0	V_{40}	1	0	0	0	0	0
V_9	0	0	1	0	0	1	V_{41}	1	0	1	0	0	1
V_{10}	0	0	1	0	1	0	V_{42}	1	0	1	0	1	0
V_{11}	0	0	1	0	1	1	V_{43}	1	0	1	0	1	1
V_{12}	0	0	1	1	0	0	V_{44}	1	0	1	1	0	0
V_{13}	0	0	1	1	0	1	V_{45}	1	0	1	1	0	1
V_{14}	0	0	1	1	1	0	V_{46}	1	0	1	1	1	0
V_{15}	0	0	1	1	1	1	V_{47}	1	0	1	1	1	1
V_{16}	0	1	0	0	0	0	V_{48}	1	1	0	0	0	0
V_{17}	0	1	0	0	0	1	V_{49}	1	1	0	0	0	1
V_{18}	0	1	0	0	1	0	V_{50}	1	1	0	0	1	0
V_{19}	0	1	0	0	1	1	V_{51}	1	1	0	0	1	1
V_{20}	0	1	0	1	0	0	V_{52}	1	1	0	1	0	0
V_{21}	0	1	0	1	0	1	V_{53}	1	1	0	1	0	1
V_{22}	0	1	0	1	1	0	V_{54}	1	1	0	1	1	0
V_{23}	0	1	0	1	1	1	V_{55}	1	1	0	1	1	1
V_{24}	0	1	1	0	0	0	V_{56}	1	1	1	0	0	0
V_{25}	0	1	1	0	0	1	V_{57}	1	1	1	0	0	1
V_{26}	0	1	1	0	1	0	V_{58}	1	1	1	0	1	0
V_{27}	0	1	1	0	1	1	V_{59}	1	1	1	0	1	1

Continued table (1)

	Sf	*Se*	*Sd*	*Sc*	*Sb*	*Sa*		*Sf*	*Se*	*Sd*	*Sc*	*Sb*	*Sa*
V_{28}	0	1	1	1	0	0	V_{60}	1	1	1	1	0	0
V_{29}	0	1	1	1	0	1	V_{61}	1	1	1	1	0	1
V_{30}	0	1	1	1	1	0	V_{62}	1	1	1	1	1	0
V_{31}	0	1	1	1	1	1	V_{63}	1	1	1	1	1	1

By using the transformation matrix of Eq.(4), the inverter phase voltages can be represented in the stationary reference frame as:

$$\begin{bmatrix} v_{ds} \\ v_{qs} \\ v_{z_1s} \\ v_{z_2s} \\ v_{o_1s} \\ v_{o_2s} \end{bmatrix} = \frac{V_{dc}}{\sqrt{3}} \begin{bmatrix} 1 & .5 & -.5 & -1 & -.5 & .5 \\ 0 & \frac{\sqrt{3}}{2} & \frac{\sqrt{3}}{2} & 0 & -\frac{\sqrt{3}}{2} & -\frac{\sqrt{3}}{2} \\ 1 & -.5 & -.5 & 1 & -.5 & -.5 \\ 0 & -\frac{\sqrt{3}}{2} & \frac{\sqrt{3}}{2} & 0 & -\frac{\sqrt{3}}{2} & \frac{\sqrt{3}}{2} \\ \frac{1}{\sqrt{2}} & -\frac{1}{\sqrt{2}} & \frac{1}{\sqrt{2}} & -\frac{1}{\sqrt{2}} & \frac{1}{\sqrt{2}} & -\frac{1}{\sqrt{2}} \\ 0 & 0 & 0 & 0 & 0 & 0 \end{bmatrix} \begin{bmatrix} S_A \\ S_B \\ S_C \\ S_D \\ S_E \\ S_F \end{bmatrix} \tag{13}$$

The 6-φ voltage source inverter has a total of 64 switching states. There are ten zero voltage states and 54 active voltage states. It must be noted that these numbers depend on the transformation matrix used. The active space voltage vectors can be represented in the *d-q* plane as shown in Fig. (2). It seems that the control flexibility will be better with this large number of states. To operate the inverter using these states, the authors have carried out many trials; however, all the trials lead to a highly distorted inverter output. To discover the core of this problem, let us investigate the circuits of Fig. (3). These five circuits are the only possible circuits of the inverter with the load at any switching state, except the zero states. Therefore, the motor phase voltages can take discrete values $\pm 1/2V_{dc}$, for Fig. (3-a), ($\pm 1/6V_{dc}$, $\pm 5/6V_{dc}$), for Fig. (3-b) & Fig. (3-c), and ($\pm 1/3V_{dc}$, $\pm 2/3V_{dc}$), for Fig. (3-d) & Fig. (3-e). This means that with any inverter switching state the inverter circuit can take one of these five circuits. For the inverter output voltage to be balanced, 60º must shift the six phase voltages. Consequently, three phases are in antiphase with the remaining three. Therefore, with balanced voltages, the instantaneous phase voltages (v_{As}, v_{Bs}, v_{Cs}) should equal the negative of (v_{Ds}, v_{Es}, v_{Fs}), respectively. However, for the 6-ϕ inverter to operate in balanced mode, the only possible switching states are those corresponding to the circuit of Fig. (3-a). Hence, the voltage vectors that can be used for balanced 6-ϕ are (V_7, V_{14}, V_{28}, V_{56}, V_{49}, V_{35}), i.e. the motor phase voltage will be $\pm 1/2V_{dc}$. Therefore, the phase voltages will contain large harmonics and the benefits of the 6-ϕ system will be lost. An improved performance can be obtained with the aid of dual 3-ϕ inverters, as shown in Fig. (3-f).

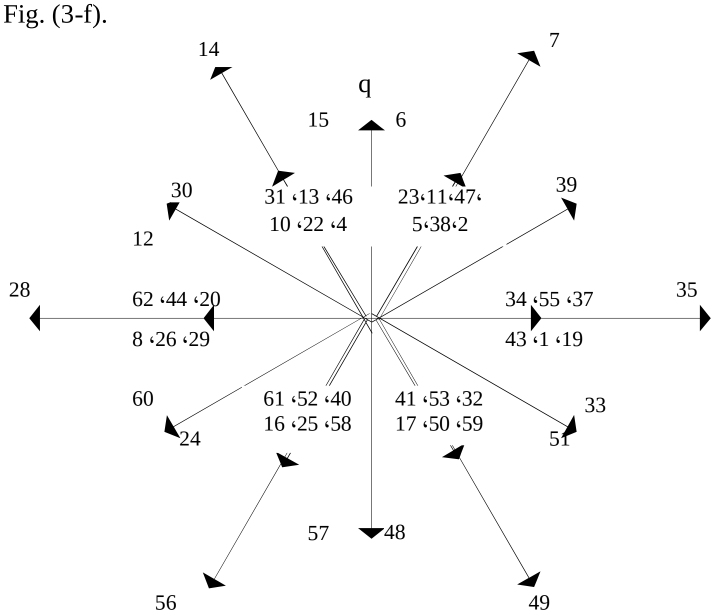

Fig. (2). Six-phase inverter states.

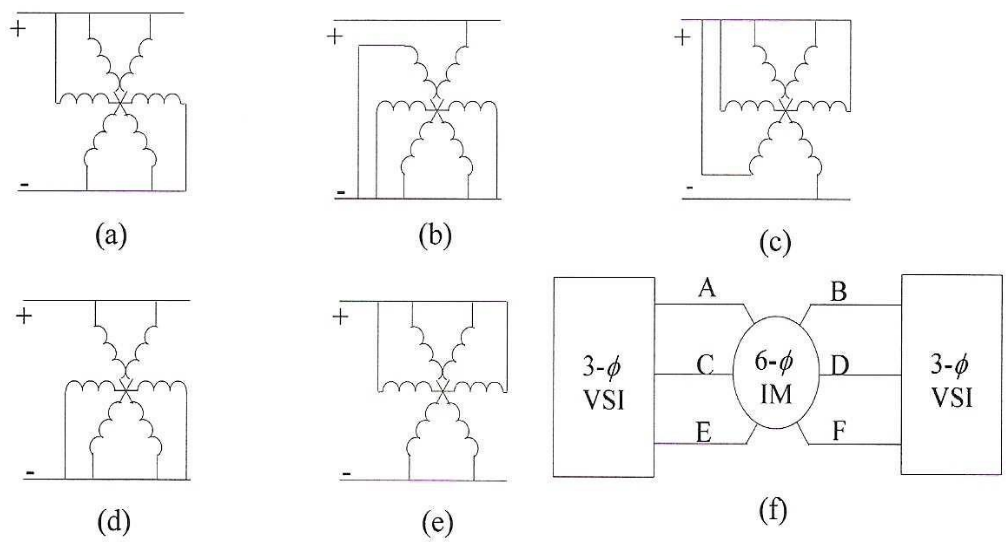

Fig. (3). (a-e)The 6-φ□inverter-motor possible circuits,(f) the dual inverter fed 6-φ□IM.

The simulated six-step operation of Fig. (4) indicates that for balanced motor operation, the inverter states must take the same previous states (V_7, V_{14}, V_{28}, V_{56}, V_{49}, V_{35}).

However, to achieve these voltage states, there must be synchronization between the two inverters signals. For instance, to get V_7 we must send a control signal to the inverters as (000111) to the legs (*F-E-D-C-B-A*). This means that the 1st inverter (*A-C-E*) must receive a control signal (110), while the 2nd (*B-D-F*) must receive a control signal (100).

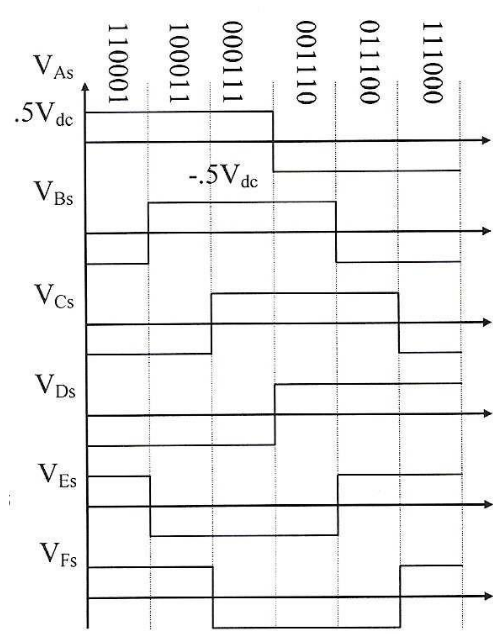

Fig. (4). The six-step operation of the 6-φ□inverter.

4. Direct Torque Control of 6-φ IM DRIVE

As the 6-φ IM model in the stationary reference frame is similar to the 3-φ one, then the principles of DTC that are essentially prepared for 3-φ IM, [13−15], can be applied to 6-φ IM. By controlling the relative motion between the stator flux and rotor flux vectors the torque can be controlled. In voltage source inverters (VSI's) that are convenient for DTC drives, the stator flux is a state variable that can be adjusted by the stator voltage and the motion of the stator flux is fully controlled by the proper selection of the stator voltage vector. The aim of DTC is to control both the flux and the torque so as to be in hysteresis band as shown in Fig. (6). For this the motion of the stator flux vector is adjusted by selecting the appropriate voltage vector. The voltage vector is selected according to the following rules:

1. Selecting an active voltage vector will move the stator flux vector, i.e. increase or decrease the flux and the torque.
2. Selecting a zero voltage vector will stop the flux vector motion, the magnitude will not change, and will decrease the torque.
3. The *d*-*q* plane, where the stator flux vector lies, is divided into six regions or sectors [13] as shown in Fig. (5). In each sector the next two adjacent voltage vectors can be selected to increase the torque and increase or decrease the flux respectively. For instance, in sector "1", either vector V_7 or V_{14} can be selected to increase the torque. However, V_7 will increase the stator flux magnitude but V_{14} will decrease the stator flux magnitude.

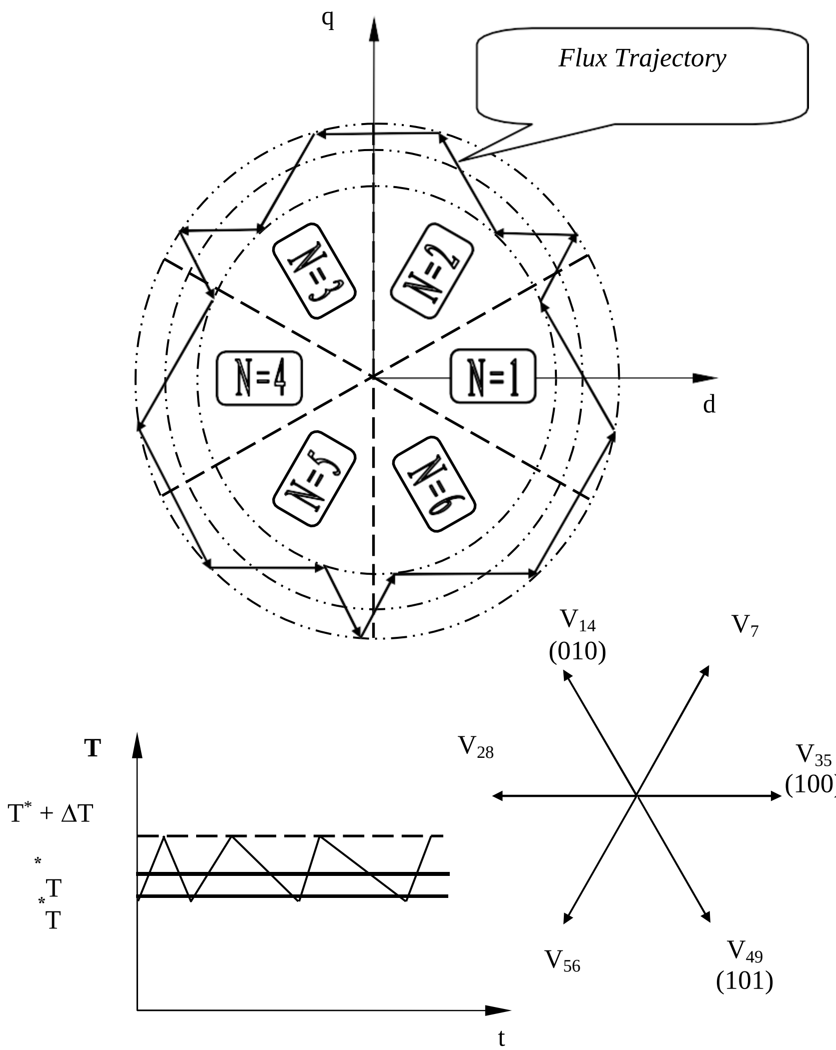

Fig. (5). Typical torque and flux (trajectory) responses with DTC.

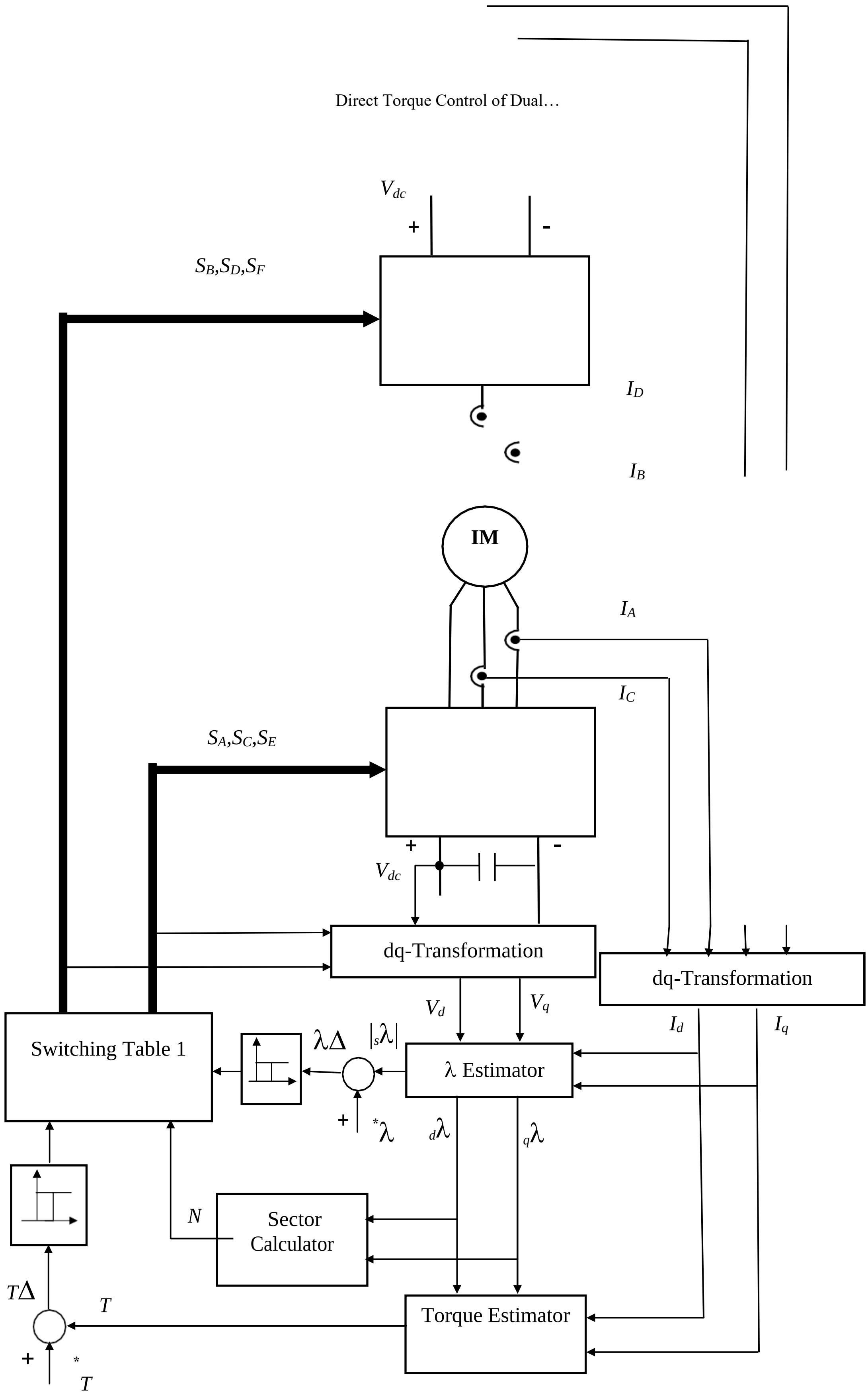

Fig. (6). Block diagram of a 6-φ IM drive controlled with DTC.

Hence, the proper voltage vector, that affects both the flux and torque in a certain sector, is known and the results can be summarized in Table (2).

Table (2). Voltage vector selection with DTC.

$\Delta\lambda$	ΔT	*N*					
		1	**2**	**3**	**4**	**5**	**6**
$\Delta\lambda = 1$	$\Delta T = 1$	V_7	V_{14}	V_{28}	V_{56}	V_{49}	V_{35}
	$\Delta T = 0$	V_{63}	V_0	V_{63}	V_0	V_{63}	V_0
$\Delta\lambda = 0$	$\Delta T = 1$	V_{14}	V_{28}	V_{56}	V_{49}	V_{35}	V_7
	$\Delta T = 0$	V_0	V_{63}	V_0	V_{63}	V_0	V_{63}

The basic block diagram of DTC system for a voltage source PWM inverter-fed IM drive is shown in Fig.(6). In this system the current and voltage vectors of the stator are measured then the real electric torque and the stator flux vector is estimated through simple estimators. The zone detector detects the sector "*N*=1….6" of the flux vector from its angle. The estimated torque is compared with the reference torque, which is the output of the speed controller, and the estimated flux is compared with the reference flux. The flux and torque controllers are hysteresis controllers which produce digitized output signals "'1' to increase and '0' to decrease".

These signals with the stator flux position signal and the sector number form the digital address to the EPROM that stores the switching Table (1). The output of the EPROM is the switching states of the inverter that form directly the control signals of the drive circuit of the inverter transistors.

5. Simulation Results

A speed control system is simulated using Matlab with a motor that has the parameters given in Table (3) [5]. A five horsepower, four poles IM with thirty-six stator slots was rewound to form a six pole, six phase IM.

Table (3). Motor parameters

N	*1150rpm*	R_s	*.71Ω*	L_s	*.05331H*
v_{ph}	*145V*	R_r	*1.29Ω*	*J*	*.05N.m.sec*^{2}
F	*60Hz*	L_m	*.0489H*	λ_s	*0.82Wb*
		L_r	*.05331H*	T_L	*8N.m*

The torque and flux step response are shown in Fig. (7). It is noted that both torque and flux are within the hysteresis bands at steady state. The motor phase currents and voltages are balanced; the phase voltage and current is shown in Fig. (8). The stator flux locus, shown in Fig. (9), nearly resembles a circle. The current spectrum of the 6-φ□motor and that of a 3-φ□motor of the same rating; at full load; are shown in Fig. (10).

It is noted from the figure that there is a third harmonic component with 6-φ drive, this is a built in disadvantage of the 6-φ IM [1]. However, the total harmonic distortion of the 6-φ drive is less than that of the 3-φ drive. The high order current harmonics appeared in the 6-φ spectrum has no effect on the motor torque as it is absorbed by the motor inertia.

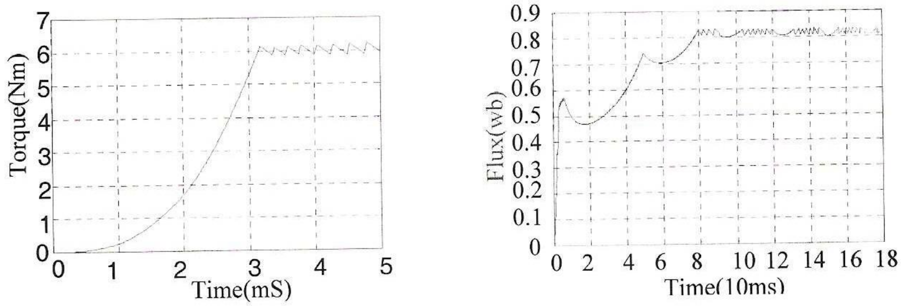

Fig. (7). Flux and torque step responses of 6-φ□IM with DTC at starting, the step torque and flux are 75% and 100% respectively.

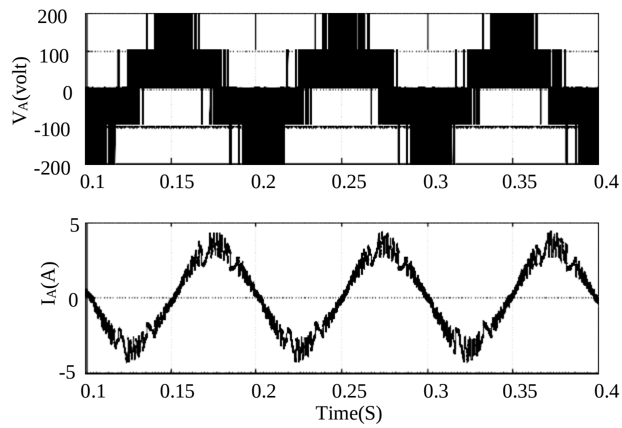

Fig. (8). Phase "A" voltage and current of 6-φ□IM with DTC at steady state,no load, and 195 rpm.

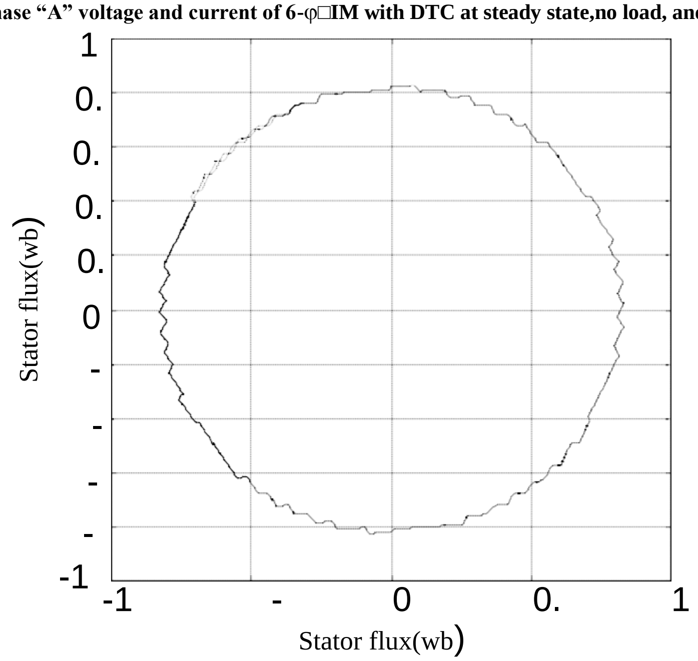

Fig. (9). Stator flux locus of 6-φ IM with DTC.

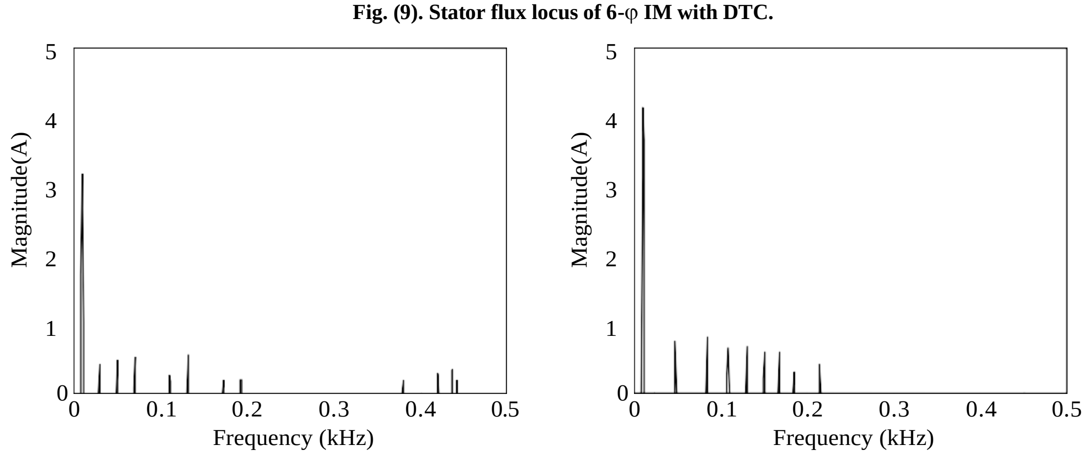

Fig. (10). Current Spectrum of DTC controlled 6-φ IM "left" and 3-φ IM "right".

6. Conclusion

Modeling and simulation of a 6-φ IM drive with DTC has been examined. The salient conclusions that emerged from the study are the following:

1. With the conventional 6-φ inverter there are 64 possible locations for the resultant voltage vector, however only 6 locations can be utilized to generate balanced output.
2. An improved performance over the results of the field orientation trials in the literature has been obtained with the aid of dual 3-φ inverters.
3. Compared to the 3-φ drive, the converter total harmonic distortion of the 6-φ drive is less than that of the 3-φ drive.

7. References

[1] Klingshirn E. A., "High phase order induction motors," *IEEE Trans. on Power Apparatus and Systems*, Vol. PAS-102, No. 1, (1983). 47-59.
[2] Abbas M. A., Christen R., and Jahns T. M., "Six-phase voltage source inverter driven induction motor," *IEEE Trans. on Industry Applicat.*, Vol. IA-20, No. 5, (1984). 1251-1259.
[3] Toliyat H. A., "Analysis and simulation of five-phase variable speed induction motor under asymmetrical connections," *IEEE Trans. on Power Elect.*, Vol. 13, No. 4, (1998). 748-756.
[4] Scholey D., "Induction motors for variable frequency power supplies," *IEEE Trans. on Industry Applicat.*, Vol. IA-18, No. 4, (1982).
[5] Zhao Y., and Lipo T. A., "Space vector PWM control of dual three-phase induction machine using vector space decomposition," *IEEE Trans. on Industry Applicat.*, Vol. 31, No. 5, (1995). 1100-1109.
[6] Gopakumar K., Ranganathan V. T., and Baht S. R., "Split-phase induction motor operation from PWM voltage source inverter," *IEEE Trans. on Industry Applicat.*, Vol. 29, No. 5, (1993). 927-932.
[7] Pavithran K. N., Parimelalagan R., and Krishnamurthy M. R., "Studies on inverter-fed five-phase induction motor drive," *IEEE Trans. on Power Elect.*, Vol. 3, No. 2, (1988). 748-756.
[8] Mohpatra K. K., Gopakumar K., Somasekhar V. T., and Umanand L., "A novel modulation scheme for a six phase induction motor winding," IECON 2002., Vol. 1, (2002). 810-815.
[9] Yazdani D., Khajehoddin S. A., Bakhshai A., and Joos G., "A generalized space vector classification technique for six phase inverters," PESC 2007, (2007). 2050-2054.
[10] Aroquiadassou G., Henao H., Capolino G. A., Boglietti A., and Cavagnino A., "A simple circuit model for predicting six-phase induction machine performances," IECON 06., Vol. 1, (2006). 1441-1446.
[11] Zhao Y., and Lipo T. A, "Modeling and control of a multi-phase induction machine with structural unbalance," *IEEE Trans. On Energy Conversion*, Vol. 11, No. 3, (1996). 570-577.
[12] White D. C., and Woodson H. H., *Electromechanical Energy Conversion*, New York: John Wiley & Sons, (1959).
[13] Takahashi I., and Noguchi T., "A new quick response and high efficiency control strategy of an induction motor," *IEEE Trans. on Industry Applicat.*, Vol. IA-22, No. 5, (1986). 820-827,.
[14] Tiitinen P., Pohjalianen P., and Lalu J., "The next generation motor control method DTC," Revue ABB, (1995) 19-24.
[15] Kazmierkowski M. P., and Kasprowicz A. B., "Improved direct torque and flux vector control of PWM inverter fed induction motor drives," *IEEE Trans. on Industrial Elect.*, Vol. 42, No. 4, (1995). 344-350,.

Appendix I

The resistance and inductance matrices in Eq.(1) and Eq.(2) are defined as follows, according to the machine structure:

The stator and rotor resistance matrices $[R_s]$, $[R_r]$:

$$[R_s]=\begin{bmatrix} R_s & 0 & 0 & 0 & 0 & 0 \\ 0 & R_s & 0 & 0 & 0 & 0 \\ 0 & 0 & R_s & 0 & 0 & 0 \\ 0 & 0 & 0 & R_s & 0 & 0 \\ 0 & 0 & 0 & 0 & R_s & 0 \\ 0 & 0 & 0 & 0 & 0 & R_s \end{bmatrix},\quad [R_r]=\begin{bmatrix} R_r & 0 & 0 & 0 & 0 & 0 \\ 0 & R_r & 0 & 0 & 0 & 0 \\ 0 & 0 & R_r & 0 & 0 & 0 \\ 0 & 0 & 0 & R_r & 0 & 0 \\ 0 & 0 & 0 & 0 & R_r & 0 \\ 0 & 0 & 0 & 0 & 0 & R_r \end{bmatrix} \qquad \text{(I-1)}$$

The stator self-inductance matrix [L_{ss}]:

$$[L_{ss}]=L_{ls}\bullet[I]+L_m\bullet\begin{bmatrix} 1 & .5 & -.5 & -1 & -.5 & .5 \\ .5 & 1 & .5 & -.5 & -1 & -.5 \\ -5 & .5 & 1 & .5 & -.5 & -1 \\ -1 & -.5 & .5 & 1 & .5 & -.5 \\ -5 & -1 & -.5 & .5 & 1 & .5 \\ .5 & -.5 & -1 & -.5 & .5 & 1 \end{bmatrix} \qquad \text{(I-2)}$$

The rotor self-inductance matrix [L_{rr}]:

$$[L_{rr}]=L_{lr}\cdot[I]+\left(\frac{N_r}{N_s}\right)^2\cdot L_m\bullet\begin{bmatrix} 1 & .5 & -.5 & -1 & -.5 & .5 \\ .5 & 1 & .5 & -.5 & -1 & -.5 \\ -.5 & .5 & 1 & .5 & -.5 & -1 \\ -1 & -.5 & .5 & 1 & .5 & -.5 \\ -.5 & -1 & -.5 & .5 & 1 & .5 \\ .5 & -.5 & -1 & -.5 & .5 & 1 \end{bmatrix} \qquad \text{(I-3)}$$

Where L_{ls}, L_{lr}, and L_m are the stator leakage, rotor leakage and mutual inductances.

$$[L_{sr}] = L_m \cdot \begin{bmatrix} c(\theta) & c(\frac{\pi}{3}+\theta) & c(\frac{2\pi}{3}+\theta) & c(\frac{3\pi}{3}+\theta) & c(\frac{4\pi}{3}+\theta) & c(\frac{5\pi}{3}+\theta) \\ c(\frac{5\pi}{3}+\theta) & c(\theta) & c(\frac{\pi}{3}+\theta) & c(\frac{2\pi}{3}+\theta) & c(\frac{3\pi}{3}+\theta) & c(\frac{4\pi}{3}+\theta) \\ c(\frac{4\pi}{3}+\theta) & c(\frac{5\pi}{3}+\theta) & c(\theta) & c(\frac{\pi}{3}+\theta) & c(\frac{2\pi}{3}+\theta) & c(\frac{3\pi}{3}+\theta) \\ c(\frac{3\pi}{3}+\theta) & c(\frac{4\pi}{3}+\theta) & c(\frac{5\pi}{3}+\theta) & c(\theta) & c(\frac{\pi}{3}+\theta) & c(\frac{2\pi}{3}+\theta) \\ c(\frac{2\pi}{3}+\theta) & c(\frac{3\pi}{3}+\theta) & c(\frac{4\pi}{3}+\theta) & c(\frac{5\pi}{3}+\theta) & c(\theta) & c(\frac{\pi}{3}+\theta) \\ c(\frac{\pi}{3}+\theta) & c(\frac{2\pi}{3}+\theta) & c(\frac{3\pi}{3}+\theta) & c(\frac{4\pi}{3}+\theta) & c(\frac{5\pi}{3}+\theta) & c(\theta) \end{bmatrix} \quad \text{(I-4)}$$

$$[L_{rs}] = L_m \cdot \begin{bmatrix} c(\theta) & c(\frac{\pi}{3}-\theta) & c(\frac{2\pi}{3}-\theta) & c(\frac{3\pi}{3}-\theta) & c(\frac{4\pi}{3}-\theta) & c(\frac{5\pi}{3}-\theta) \\ c(\frac{5\pi}{3}-\theta) & c(\theta) & c(\frac{\pi}{3}-\theta) & c(\frac{2\pi}{3}-\theta) & c(\frac{3\pi}{3}-\theta) & c(\frac{4\pi}{3}-\theta) \\ c(\frac{4\pi}{3}-\theta) & c(\frac{5\pi}{3}-\theta) & c(\theta) & c(\frac{\pi}{3}-\theta) & c(\frac{2\pi}{3}-\theta) & c(\frac{3\pi}{3}-\theta) \\ c(\frac{3\pi}{3}-\theta) & c(\frac{4\pi}{3}-\theta) & c(\frac{5\pi}{3}-\theta) & c(\theta) & c(\frac{\pi}{3}-\theta) & c(\frac{2\pi}{3}-\theta) \\ c(\frac{2\pi}{3}-\theta) & c(\frac{3\pi}{3}-\theta) & c(\frac{4\pi}{3}-\theta) & c(\frac{5\pi}{3}-\theta) & c(\theta) & c(\frac{\pi}{3}-\theta) \\ c(\frac{\pi}{3}-\theta) & c(\frac{2\pi}{3}-\theta) & c(\frac{3\pi}{3}-\theta) & c(\frac{4\pi}{3}-\theta) & c(\frac{5\pi}{3}-\theta) & c(\theta) \end{bmatrix} \quad \text{(I-5)}$$